

Introduction to Simultaneous Location and Mapping Algorithm based on Point-line Matching

Zhongbo Wang^a, Wenhua Cui^{*}, Ye Tao^b, and Tianwei Shi^c

School of Computer and Software Engineering, University of Science and Technology Liaoning, Anshan, 114051, China

^a15842021418@163.com, ^{*}cwh@systemteq.net, ^btaibeijack@163.com, ^ctianweiabbcc@163.com

Abstract

Robot technology is becoming more and more influential in people's life. Robot positioning and acquiring surrounding information and building maps are important parts of the research and development of robot technology. This paper first introduces the development of the positioning and built figure technology background, then the laser radar sensor and its working principle, tells the story of the laser radar since movement distortion causes and solutions, and finally describes the acquisition of laser radar point cloud data processing method including segmentation of point cloud and almost to remove, Clustering method after point cloud data segmentation and matching method of two continuous point cloud frames based on point line matching.

Keywords

Robotics; Simultaneous Positioning and Mapping; Point-Line Matching.

1. Introduction

In recent years, with the development of artificial intelligence technology, robot technology has also achieved rapid development. Robot technology has been applied in various fields, and the development of robot technology has brought great convenience to people's life. The simultaneous positioning and mapping technology is the premise of the development of robot technology. Before the robot needs to complete navigation and obstacle avoidance tasks, the robot first needs to complete its own positioning and establish a map of the surrounding environment in a way that the robot can recognize.

Using laser radar to complete robot localization and built figure is the orientation and at the same time build a hot direction of the graph problem, laser radar by patch cloud data passed to the location and at the same time build graph algorithm for continuous laser radar position estimation between frames, get laser radar posture change between consecutive frames, the initial position to the laser radar movement map is established with the origin of coordinates. The point line matching method is an excellent method of lidar point cloud frame matching, so this paper describes the simultaneous positioning and mapping algorithm based on the point line matching method.

2. Lidar Model

2.1 Introduction to Lidar

As a kind of high-precision sensor, lidar is widely used in robot, unmanned driving and other scenarios because it can output the distance information from the surrounding environment conveniently and reliably. The research of high performance laser SLAM has been the pursuit of academia and industry. Lidar can be divided into 2D lidar and 3D lidar according to its laser scanning

range [1]. Accordingly, THE SLAM algorithm based on lidar is also divided into 2D laser SLAM algorithm and 3D laser SLAM algorithm. 3D laser SLAM algorithm provides more information than 2D laser SALM because it can build a dense 3D model of the environment. It can not only achieve 6-DOF pose estimation [2], but also provide more information related to the real world for navigation planning, such as the size, distance and even category of objects in the scene. Therefore, it has a very broad application prospect.

2.2 Lidar TOF Ranging Principle

The TOF principle uses the speed of light to range. First, a laser emitter emits a laser pulse, and a timer records the launch time. The pulse is received by the receiver after being reflected by the object, and the timer records the receiving time; The time difference is multiplied by the speed of light to get twice the distance [3]. As shown in Figure 1, the LiDAR TOF principle ranging example diagram.

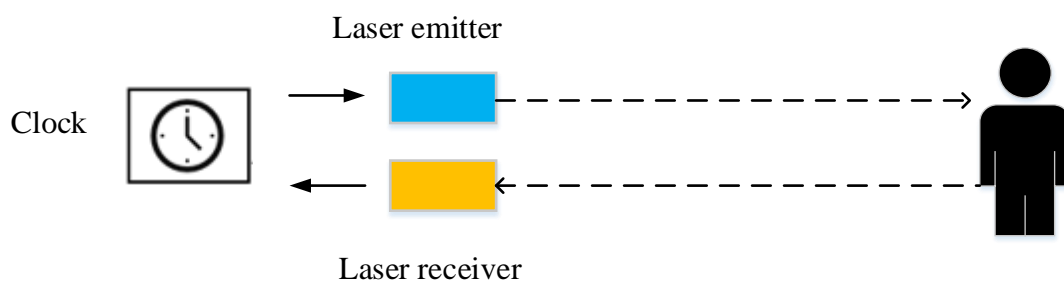


Figure 1. LiDAR TOF principle ranging example

3. A Method of Lidar Motion Distortion Removal

3.1 The Point Cloud Data

SLAM attempts to solve the problem of how to determine the trajectory of a robot moving in an unknown environment by observing the environment and at the same time build a map of the environment. Under normal circumstances, aiming at the problem of simultaneous positioning and mapping of robots, the system created is usually composed of three parts: front end, back end and loop detection. Sensor information in LASER SLAM is mainly read and preprocess of lidar information, and this paper also includes read and process of IMU data.

3.2 Self-motion Distortion of Lidar

For most lidar, although the laser is emitted and received quickly, each point that makes up the point cloud is not created at the same time. Generally, the data accumulated within 100ms (corresponding to the typical value of 10Hz) is output as a frame point cloud. If the absolute position of the lidar body or the body on which it is installed changes in the 100ms, then the coordinate system of each point in the frame cloud is different. Intuitively, this frame of point cloud data will undergo certain "deformation", which cannot truly correspond to the detected environmental information, similar to the hand shaking when taking a photo, the photo will be blurred. This is the self-motion distortion of lidar [4]. As shown in Figure 2 below, when the lidar receives the transmitted signal to obtain point cloud data, the optimal effect is shown on the left, that is, the position of the lidar does not change from that at the end of the scanning to obtain point cloud data, but the actual effect is shown on the right. The position of the lidar will change from the beginning of the scanning to the end of the scanning, so that the point cloud data obtained are not in the same coordinate system. It will cause large error to build a map based on the frame point cloud data.

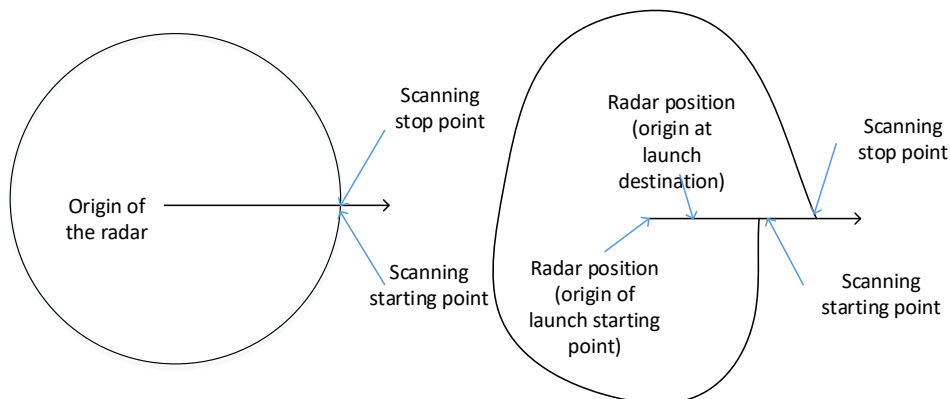


Figure 2. self-motion distortion of 360-degree mechanical lidar

In essence, the distortion of lidar point cloud is caused by the difference of coordinate system of each point in a frame. In Figure 3 below, $p_1 \sim p_3$ on the left represent the three position points scanned by lidar in turn, which are aligned in the real world. However, because the lidar itself has "violent" movement within a frame, as shown in the middle figure, the radar itself scans the three points under three different actual attitudes. So in the resulting point cloud (far right), the coordinates of the three points are actually in different coordinate systems and no longer look collinear.

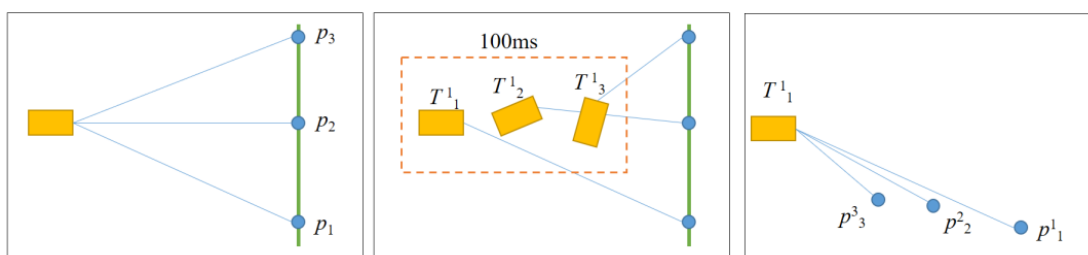


Figure 3. Changes in point cloud coordinate system

3.3 A method for Removing Movement Distortion of Lidar

The distortion of point cloud is caused by the movement of radar carrier in the process of data collection of a frame. Therefore, it is necessary to calculate the movement of radar in the process of data collection first, and then compensate this movement according to the relative time of each point in each frame, including the compensation of rotation and translation. The methods of point cloud distortion include pure estimation method (ICP/VICP), sensor-assisted method (IMU/ODOM) and fusion method [5-7].

Among them, IMU sensor-assisted method is used: IMU provides the velocity, acceleration and other information of the carrier, and the carrier can be assumed as a uniform velocity motion model in the low-speed motion scene, that is, coordinate = motion \times time. In the scene of high-speed motion, IMU information can also be used to correct the error of the non-uniform part assumed by the uniform speed model [8].

The time of radar scanning a frame is fixed, and the acquisition time of each point is obtained through calculation, so that all points are unified at the same time. Suppose that the end time of each frame scanning is selected, as shown in Figure 4 below:

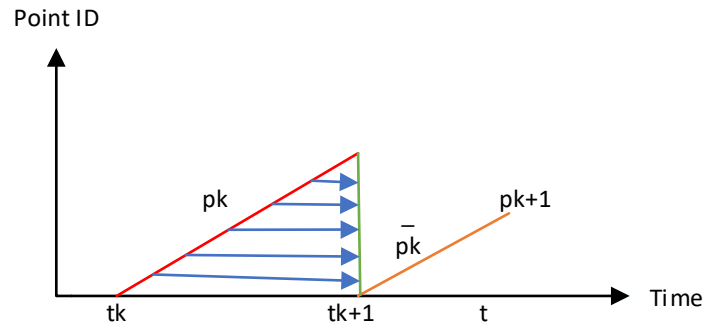


Figure 4. Calculation of radar scanning time

The ordinate Point ID is the frame number of Point cloud, the ordinate Time is the radar scanning Time, t_k is when a frame scan starts, t_{k+1} is the end of a scan, $t_{k+1} - t_k$ is the fixed scanning time, the horizontal arrow represents the projection of all points to time t_{k+1} . \bar{p}_k is the point cloud generated by this frame scan, and obviously different points have different timestamps. The relative position and pose of the radar at time t_{k+1} relative to time t_k was denoted as T_{k+1}^L , and its compensation transformation matrix $T_{(k+1,i)}^L$ was calculated for each point, as shown in the formula below, and simple linear interpolation was performed

$$T_{(k+1,i)}^L = \frac{t_i - t_{k+1}}{t_k - t_{k+1}} T_{k+1}^L \quad (1)$$

The specific steps are as follows: First, synchronize the lidar and IMU, obtain the IMU data closest to the time stamp of a frame point cloud according to the time stamp of the lidar and IMU, subtract the time stamp to calculate the travel value, and if the time difference is less than the synchronization threshold, the data is output as synchronization data. If the time difference is greater than the synchronization threshold, the data is discarded, and a frame of lidar sampling data is taken down and the above process is repeated. Then, the disordered point cloud is transformed in order. Take PVP-16 as an example, a frame of DATA of PVP-16 is output in the form of point cloud (i.e., a bunch of points, each point has information of XYZ, and there is no other relational information between points), so we don't know which Scan each point belongs to and which horizontal Angle it corresponds to. Therefore, a single frame point cloud needs to be divided into line bundles (divided into 16 bundles), and the line bundles to which each point belongs and the relative scanning time of each point in this frame point cloud (relative to the first point in this frame) are recorded. After that, the carrier motion information was calculated to obtain the Euler Angle of the three axes relative to the world coordinate system and the acceleration on the three axes in the IMU coordinate system. Then, the acceleration of IMU in the world coordinate system was obtained by removing the influence of gravity, and the corresponding displacement and velocity of each IMU data frame in the world coordinate system were obtained. Finally, the compensation transformation matrix of each laser point relative to the initial point is calculated by interpolation with the obtained motion information. Finally convert each laser point. For each laser point, the corrected laser point coordinates can be obtained by multiplying the compensation transformation matrix by the original laser point coordinates [9-11].

4. Point Cloud Segmentation and Handicap Removal

4.1 Point Cloud Recording Method

For a frame of point cloud information input by lidar, including n-line point cloud data, the input time stamp will be recorded, and the n-line point cloud data will be divided into N pieces of 1-line point cloud data, and the 1-line point cloud data will be divided into M pieces of 1-line point cloud data, and the number of point cloud M will be recorded. Finally, the system will record the offset in the X direction, Y direction, Z direction and reflection intensity of each point cloud in detail, and the reflection intensity reflects the distance between the changed point and the radar. Point cloud processing is shown in Figure 5 below.

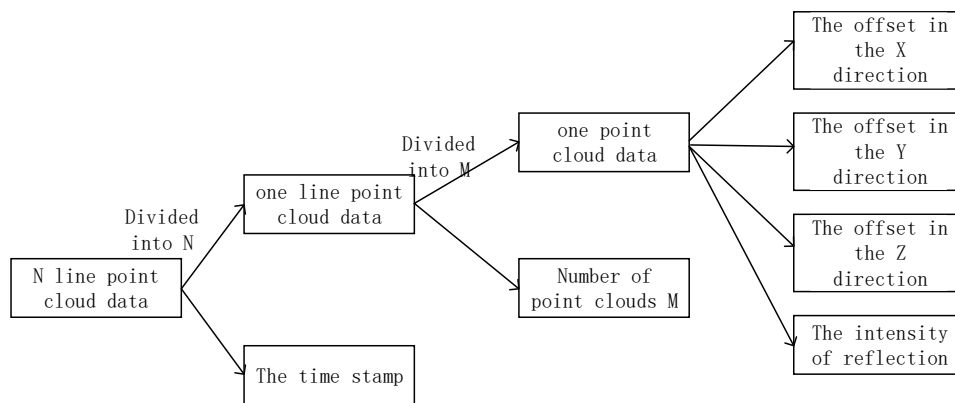


Figure 5. Point cloud recording method

4.2 Point Cloud Segmentation and Clustering

Firstly, point cloud segmentation is performed on the original point cloud input. The main process of point cloud segmentation is first ground extraction, then segmentation of the remaining point clouds, and finally the segmented point cloud is carried out for the next step of feature extraction. Firstly, the

point cloud obtained at time T is $P_t \{p_1, p_2, p_3, \dots, p_n\}$. p_i is a point in the point cloud P_t at time t . The point cloud is projected into a range image with a resolution of 1800×16 . Since the horizontal angular resolution of THE VLP-16 is 0.2° , the horizontal resolution of the projected image is $360/0.2=1800$. Since the vertical direction of THE VLP-16 is 16 scan lines, the vertical resolution of the projected image becomes 16. After the point cloud is projected onto the image, each point in three-dimensional space becomes a pixel in two-dimensional space, obtain the Euclidean distance r_i

between pixel point P_i and sensor. Before segmentation, the progressive of the distance image is evaluated and ground points are extracted [12]. Since the vertical direction of the distance is 16, this also represents the properties of the vertical dimension in the original three-dimensional space. Therefore, ground points and non-ground points can be well marked by judging the characteristics of their vertical dimension. The range of the laser scanning beam through THE VLP-16 is $[-15^\circ, 15^\circ]$, and the ground point must appear on the scan line $[-15^\circ, -1^\circ]$. In this process, marked ground points can be removed from subsequent segmentation.

4.3 Point Cloud Clustering

The distance image is segmented into many clusters by image - based segmentation method. Points in the same cluster are marked with unique identifiers. In this step, some small object points can be removed as noise points to reduce the interference caused by the non-repeated appearance of small objects between adjacent frames: leaves and grass floating in the wind are often encountered in practical experiments, which may cause the situation that they appear in the previous frame but not in the later frame. Removing the point cloud that cannot be clustered can reduce the interference of

noise points and improve the feature extraction accuracy on the basis of retaining the feature information of the current frame [13].

In order to improve the processing efficiency, all the categories with less than 30 data points are treated as noise points, so that some relatively static objects (such as tree trunks, buildings, etc.) are preserved. In this way, the whole distance image can be divided into several larger categories. Add the previous set of a category - ground points, so you can proceed. Based on the processing in this step, points in a point cloud frame can be removed many noise points, as shown in Figure. 6 below:

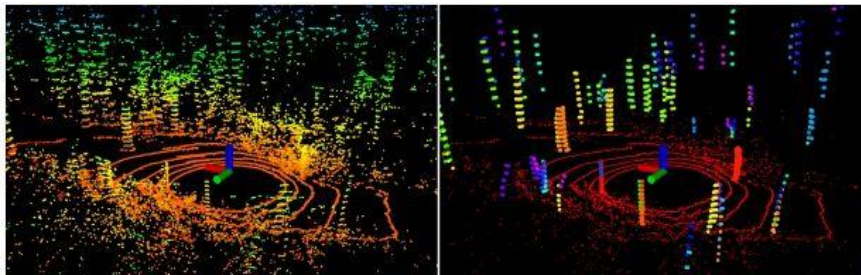


Figure 6. Point cloud noise processing comparison diagram

As you can see from the figure, most of the messy points have been removed by processing, leaving the data to be processed clean. Based on this step, the following three information can be obtained for each point: the segmentation label (ground point or segmentation point), the index of rows and columns in the distance image and the distance value r_i of the sensor.

5. Point Cloud Matching

For front-end scan matching, representative 3D point cloud matching algorithms can be roughly divided into two categories: matching based method and feature based method. The objective evaluation function established based on the algorithm can be divided into two kinds: distance judgment and probabilistic model judgment. The probabilistic model judgment methods are mainly Normalized Distribution Transform (NDT) algorithm [14]. The methods based on distance judgment are mainly ICP algorithm and its variants. The algorithms suitable for 3D lidar SLAM include PP-ICP[15], NICP[16], IMLS-ICP[17], etc. The representative algorithm is GICP(Generalized Iterative Closest Point)[18]. The algorithm principle is to combine ICP algorithm and PL-ICP algorithm to the probabilistic framework model for Point cloud registration, which improves the applicability and accuracy of the algorithm. Matching algorithm generally achieves accurate estimation by directly using scanning points, which requires a large number of points for stable registration. Although the matching accuracy is high, the calculation efficiency is usually not high.

Features-based methods improve computational efficiency by extracting feature points from scanned point clouds [19], including Lego-LoAM using corner and flat point features and 3D raster matching algorithm Multi-resolution Surfel Map using surface element features [20]. In this paper, the feature matching method used in LeGO-LoAM is adopted, which is more efficient than the feature-based method based on matching method.

5.1 Feature Extraction

The remaining points after segmentation are fed into the feature extraction module for subsequent feature extraction. In order to evenly extract features from all directions, the distance image is horizontally divided into several equal sub-images, and 360° is evenly divided into 6 equal parts. For each sub-image, the following processing is carried out:

Select a point p_i in point cloud P_t at time t, find 5 points on the left and right in the same vertical direction of point p_i , construct a set S, and calculate the smoothness of each point. The smoothness formula is as follows:

$$c = \frac{1}{|S| \cdot r_i} \sum_{j \in S, j \neq i} (r_j - r_i) \quad (2)$$

After obtaining the index of smoothness, feature points can be divided into two categories: plane points and edge points. Flat point: a point on a flat plane in three-dimensional space that has little difference in size from the surrounding points, low curvature and smoothness. Edge point: a point on a sharp edge in three-dimensional space, with a large difference in size between it and the surrounding points, high curvature and smoothness. In this paper, the points in the set are sorted to find the smallest point C_{\min} as the plane point and the largest point C_{\max} as the edge point. Specific operations are as follows:

For the smoothness sorted out, the feature points are selected. Set smoothness threshold C_{th} , edge point $c > C_{th}$, plane point $c < C_{th}$. According to the above evaluation criteria, divided out of the edge point and point. nF_e edge points that do not belong to ground points and have the maximum C value are selected from each row to form the set F_{me} . Select nF_p plane points with minimum C value from each row, which can be ground points or segmentation points, to form the set F_p . After this step, the following relationship can be obtained. The point cloud diagram of feature points is extracted as shown in Figure 7:

$$F_e \subset F_{me} \ \& \ F_p \subset F_{mp} \quad (3)$$

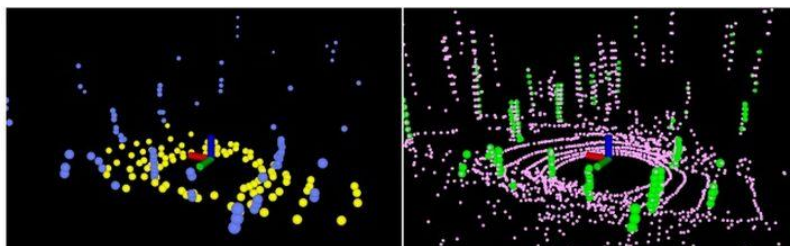


Figure 7. Example of feature points

On the left are fewer feature points, and on the right are more feature points in the front feature extraction part. Four point cloud types are obtained: $\{F_e, F_{me}, F_p, F_{mp}\}$. If the current time is set to t, the previous time is set to t-1. In order to better obtain the attitude transformation relationship between t moment and t-1 moment, in this paper, the characteristic points F_e^t and F_p^t at time t and F_{me}^{t-1} and F_{mp}^{t-1} at time t-1 are selected.

Because of $F_e \in F_{me} \ \& \ F_p \in F_{mp}$, we can definitely find the correlation between F_e^t and F_p^t from F_{me}^{t-1} and F_{mp}^{t-1} . Construct a point-to-line correspondence for $\{F_e^t, F_{me}^{t-1}\}$, and a point-to-face correspondence for $\{F_p^t, F_{mp}^{t-1}\}$. However, LEGO-LOAM has made some improvements to improve

the accuracy and efficiency of matching, mainly in two aspects: tag matching; Two-step LM optimization.

5.2 Label Matching

In the previous segmentation module, the point cloud was divided into ground points and segmentation points, and these labels were used to search the corresponding associated points. For edge points: search for the corresponding correlation point of F_e^t in the point cloud F_{me}^{t-1} with segmentation point label; for plane points: search for the corresponding correlation point of F_p^t in the point cloud F_{mp}^{t-1} with ground point label.

This step has the following two advantages: ground information is basically unchanged in the adjacent frames, and the point cloud is divided into several blocks after clustering, which reduces the candidate range of corresponding points. However, in actual experiments, if the ground is not particularly flat, that is, the ground between adjacent frames changes to a certain extent, LEGO-LOAM cannot run well. After obtaining the correspondence between point-to-line and point-to-surface, leven berg-Marquardt optimization method [21] is needed to optimize and solve the problem.

5.3 Two-step LM optimization

LM optimization methods will be carried out twice for 6-dof $([t_x, t_y, t_z, t_{roll}, t_{pitch}, t_{yaw}])$: the corresponding point constraints of $\{F_p^t, F_{mp}^{t-1}\}$ will be optimized to obtain $[t_z, t_{roll}, t_{pitch}]$. The corresponding point constraint of $\{F_e^t, F_{me}^{t-1}\}$ is optimized, and based on the $[t_z, t_{roll}, t_{pitch}]$ obtained in the first step, the two-step calculation of $[t_x, t_y, t_{yaw}]$ has definite rationality:

Since the ground remains essentially unchanged between adjacent frames, the vertical dimension variation $[t_z, t_{roll}, t_{pitch}]$ can be calculated using the point-to-surface constraint. When the vertical dimension change is calculated, the initial value can be input into the optimization of the second step to reduce the number of iterations, and the horizontal dimension change $[t_x, t_y, t_{yaw}]$ can be calculated to improve the calculation efficiency. Finally, the 6-dof attitude transformation matrix $([t_x, t_y, t_z, t_{roll}, t_{pitch}, t_{yaw}])$ is obtained based on two-step LM optimization.

6. Conclusion

This paper describes the development significance of the technology of simultaneous location and mapping, and explains the method of using lidar for simultaneous location and mapping in detail. Laser radar model and its working principle were introduced at first, then analyzes the lidar cause the distortion of the point cloud movement, this paper expounds the method to remove the distortion of the point cloud, and the segmentation of point cloud data and almost remove illustrated, finally explains how to use the method to estimate the point line matching two point cloud between changes of the laser radar pose.

Acknowledgments

This research is supported by Iot and AI Innovation Team Liaoning(601009889-04), Joint fund project of National Natural Science Foundation of China(U1908218), and Department of Education of Liaoning Province (2020FWDF01).

References

- [1] Raj T, Hashim F H, Huddin A B, et al. A survey on LiDAR scanning mechanisms. (Electronics),Vol. 9(2020)No.5,p.741-742.

- [2] Li Y, Ibanez-Guzman J. Lidar for autonomous driving: The principles, challenges, and trends for automotive lidar and perception systems. (IEEE Signal Processing Magazine), Vol.37(2020), No.4, p.50-61.
- [3] Ye H, Chen Y, Liu M. Tightly coupled 3d lidar inertial odometry and mapping(2019 International Conference on Robotics and Automation, 2019) p.3144-3150.
- [4] Liu J, Sun Q, Fan Z, et al. TOF lidar development in autonomous vehicle(2018 IEEE 3rd Optoelectronics Global Conference ,2018), p.185-190.
- [5] Ma X, Yao X, Ding L, et al. Variable motion model for lidar motion distortion correction(Optical Sensing and Imaging Technology, SPIE, 2021). p.12065: 489-495.
- [6] Wang J, Zhu H, Liu H, et al. Lossy point cloud geometry compression via end-to-end learning(IEEE Transactions on Circuits and Systems for Video Technology), Vol.31(2021), No.12, p.4909-4923.
- [7] Sun W, Wang J, Jin F, et al. A quality improvement method for 3D laser slam point clouds based on geometric primitives of the scan scene(International journal of remote sensing), Vol.42(2021), No.1, p.378-388.
- [8] Li M, Zhu H, You S, et al. Efficient laser-based 3D SLAM for coal mine rescue robots(IEEE Access), Vol.7(2018), p.14124-14138.
- [9] Xuexi Z, Guokun L, Genping F, et al. SLAM algorithm analysis of mobile robot based on lidar(2019 Chinese Control Conference ,China, 2019). p.4739-4745. (In Chinese).
- [10] Van Nam D, Gon-Woo K. Solid-state LiDAR based-SLAM: A concise review and application(2021 IEEE International Conference on Big Data and Smart Computing ,2021). p.302-305.
- [11] Akiyama N, Nishiyama S, Sakita K, et al. River Levees Monitoring Using Three Dimensional Laser Point Clouds with SLAM Technology(Civil Infrastructures Confronting Severe Weathers and Climate Changes Conference, Springer, Cham, 2021). p.14-22.
- [12] Ye S, Chen D, Han S, et al. Learning with Noisy Labels for Robust Point Cloud Segmentation (Proceedings of the IEEE/CVF International Conference on Computer Vision) p.6443-6452.
- [13] Zhang Z, Dai Y, Sun J. Deep learning based point cloud registration: an overview(Virtual Reality & Intelligent Hardware), Vol.2(2020), No.3, p.222-246.
- [14] Srinara S, Lee C M, Tsai S, et al. Performance Analysis of 3D NDT Scan Matching for Autonomous Vehicles Using INS/GNSS/3D LiDAR-SLAM Integration Scheme(2021 IEEE International Symposium on Inertial Sensors and Systems ,2021),.1-4.
- [15] Zhang S, Guo Y, Zhu Q, et al. Lidar-IMU and wheel odometer based autonomous vehicle localization system(2019 Chinese Control And Decision Conference ,2019), 4950-4955.
- [16] Serafin J, Grisetti G. NIPC: Dense normal based point cloud registration(2015 IEEE/RSJ International Conference on Intelligent Robots and Systems ,2015), p.742-749.
- [17] Tian Y, Liu X, Li L, et al. Intensity-assisted ICP for fast registration of 2D-LIDAR(Sensors) Vol.19 (2019), No.9, p.2124.
- [18] Koide K, Yokozuka M, Oishi S, et al. Globally Consistent 3D LiDAR Mapping With GPU-Accelerated GICP Matching Cost Factors(IEEE Robotics and Automation Letters), Vol.6(2021), No.4, p.8591-8598.
- [19] Jadi S, WANG K A I, ZHOU J U N, et al. Extracting Crown Morphology with a Low-Cost Mobile LiDAR Scanning System in the Natural Environment(Sains Malaysiana), Vol.50(2021), No.11, p.3193-3204.
- [20] Schöps T, Sattler T, Pollefeys M. Surfelmeshing: Online surfel-based mesh reconstruction(IEEE transactions on pattern analysis and machine intelligence), Vol.42(2019), No.10, p.2494-2507.
- [21] Lin J, Zhang F. Loam livox: A fast, robust, high-precision LiDAR odometry and mapping package for LiDARs of small FoV(2020 IEEE International Conference on Robotics and Automation, 2020), p.3126-3131.